Manipulability of Wheeled Mobile Manipulators: Application to Motion Generation

B. Bayle, J. -Y. Fourquet and M. Renaud

The International Journal of Robotics Research 2003; 22; 565
DOI: 10.1177/02783649030227007

B. Bayle
LSIIT
Strasbourg, France
bernard@eavr.u-strasbg.fr

J.-Y. Fourquet
ENIT
Tarbes, France
fourquet@enit.fr

M. Renaud
LAAS-CNRS
Toulouse, France
renaud@laas.fr

Manipulability of Wheeled Mobile Manipulators: Application to Motion Generation

Abstract

We propose a systematic modeling of the nonholonomic mobile manipulators built from a robotic arm mounted on a wheeled mobile platform. We use the models derived to generalize the standard definition of manipulability to the case of mobile manipulators. The effects of mounting a robotic arm on a nonholonomic platform are shown through the analysis of the manipulability thus defined. Several applications are evoked, particularly applications to control. The optimization of criteria inherited from manipulability considerations are given to generate the controls of our system when its end effector motion is imposed.

KEY WORDS—mobile manipulation, manipulability, nonholonomy, motion planning

1. Introduction

Nowadays, *mobile manipulator* is a widespread term which refers to robots built from a robotic arm mounted on a mobile platform. Such systems allow the most usual missions of robotic systems which require both *locomotion and manipulation* abilities (Arai 1996; Khatib 1997). Actually, such systems combine the advantages of mobile platforms and robotic arms and reduce their drawbacks. For instance, the mobile platform extends the workspace, while the arm offers many operational functionalities (simply opening a door for the robot). So, they seem particularly suited for field and service robotics. Although quite old in the robotics history (Pavlov and Timofeyev 1976), this concept has mainly been studied for less than 15 years (Dubowsky and Tanner 1988; Liu and Lewis 1990; Pin and Culioli 1990).

The publications devoted to these systems are numerous—see, for example, Bayle, Fourquet, and Renaud (2001a) for a survey—and cover a wide range of research areas. The classification of the various contributions is made difficult by the poor description of the original problems related to mobile manipulation. Among these contributions, we can classify some major concerns:

- control (Cameron, MacKenzie, and Ward 1993; Chong et al. 1997; Chung, Velinsky, and Hess 1998; Dong, Xu, and Wang 2000; Hootsmans and Dubowsky 1991; Huang, Sugano, and Tanie 2000; Liu and Lewis 1990; Pissard-Gibolet 1993), optimal control (Desai et al. 1996; Lee, Kim, and Cho 1996), elastic band (Brock and Khatib 1997; Quinlan 1994);
- path optimization problems (Carriker, Khosla, and Krogh 1991; Chen and Zalzala 1997; Pin, Culioli, and Reister 1994; Pin et al. 1997; Zhao, Ansari, and Hou 1994);
- operational motion planning problem (Seraji 1993, 1998), generalized motion planning problem (Foulon, Fourquet, and Renaud 1998), operational path planning problem (Foulon, Fourquet, and Renaud 1998, 1999) or generalized path planning problem (Bayle, Fourquet, and Renaud 2000a; Foulon, Fourquet, and Renaud 1999; Fourquet and Renaud 1996);
- dynamic modeling (Dubowsky and Tanner 1988; Fukuda et al. 1992; Inoue, Miyamoto, and Okawa 1996;

The International Journal of Robotics Research
Vol. 22, No. 7–8, July–August 2003, pp. 565-581,

Yamamoto and Yun 1996, 1997), stability, effects of mechanical disturbances (Huang, Sugano, and Tanie 1998, 2000; Rey and Papadopoulos 1997);

- multi-robot cooperation (Desai and Kumar 1996; Hashimoto, Oba, and Zenitani 1995; Khatib et al. 1996; Sugar and Kumar 1999), etc.

In spite of the great number of studies, quite few efforts have been made on the *systematic modeling* of the mobile manipulators. Among the works on the modeling of a *particular mobile manipulator*, we can cite Yamamoto and Yun (1994, 1997) and Tchoń and Muszyński (2000). There is a simple explanation for this. Indeed, if the systematic modeling of robotic arms is well known, this is not necessarily the case for mobile platforms.

In the case of *wheeled* mobile platforms, which include a large part of the land mobile manipulators, except mainly humanoids and all-terrain systems, the *rolling without slipping* (r.w.s.) of the wheels on the ground introduces specific difficulties in the modeling. The platform, which cannot move instantly in any arbitrary direction, is then said to be *nonholonomic*. If we restrict our study to that large category of wheeled mobile platforms, we must evoke the excellent contribution of Campion, Bastin, and D'Andréa-Novel (1996), which offers good tools for the generic modeling of robotic systems built from wheeled mobile platforms. We propose this modeling in this paper after we introduce the kinematic modeling of the subsystems: platform and robotic arm. This is the purpose of Section 2. This reveals, in particular, the existence of the control of mobility of the mobile manipulator, which represents the control producing instantaneous velocities of the end effector (EE) of the mobile manipulator. Also we obtain the *instantaneous kinematic location model* (IKLM) of the mobile manipulator, which sets the derivative of the EE location as a function of the control of mobility.

The previous modeling is then used in Section 3 to extend the theory of manipulability of Yoshikawa (1985), proposed for the robotic arms, to the case of wheeled mobile manipulators. This proves a very appropriate tool to characterize their instantaneous kinematics.

Section 4 points out some possible applications of this instantaneous kinematic analysis, particularly from a control point of view. Notably we address the operational motion planning problem (Bayle, Fourquet, and Renaud 2000b). Since our system is redundant, the inversion of the IKLM of the mobile manipulator allows us to solve this problem and, in the meantime, to take into account an additional criteria based on a measure of the mobile manipulator manipulability.

This study aims at understanding the use of manipulability, usually defined for robotic arms, in the case of nonholonomic mobile manipulators.

2. Modeling

In this section, we illustrate the generic modeling of the mobile manipulator using the example of a planar mobile manipulator, represented in Figure 1. We first model independently its platform in Section 2.1 and its robotic arm in Section 2.2. The modeling of the mobile manipulator will be finally established in Section 2.3.

As we will see later, the ellipsoids of manipulability are six-dimensional in the most general case. For obvious reasons of visualization and thus of pedagogy, we only provide examples of planar systems in this paper; in this case, the ellipsoids of manipulability are simple ellipses. Nevertheless, the techniques of modeling and manipulability analysis detailed here are absolutely general and thus apply to systems with more complex structures. For instance, they were successfully applied to the mobile manipulator of the LAAS. This mobile manipulator is built from a two independently driven wheel mobile platform and a six revolute joint robotic arm (Bayle, Fourquet, and Renaud 2002).

2.1. Wheeled Mobile Platform Case

Wheeled mobile platforms are properly described and modeled by Campion, Bastin, and D'Andréa-Novel (1996). In this section, we introduce only the elements which are necessary in our study. Only minor changes have been done purposely to be consistent with the modeling of mobile manipulators.

2.1.1. Description

We assume that the mobile platform moves on a planar horizontal surface. Let $\mathcal{R} = (O, \vec{x}, \vec{y}, \vec{z})$ be any fixed frame with $\vec{z}$ vertical and $\mathcal{R}' = (O', \vec{x}', \vec{y}', \vec{z}')$ a mobile frame linked to the platform. The origin of $\mathcal{R}'$ is usually chosen as a remarkable point of the platform (e.g., the midpoint of the rear axle).

The *location*[1] (Fourquet and Renaud 1999) *of the platform* is given by a vector $\boldsymbol{\xi}_p$ of $m_p = 3$ coordinates which define the position and the orientation of the platform in $\mathcal{R}$. They are called the *operational coordinates of the platform*. We write $\boldsymbol{\xi}_p = [x\ y\ \vartheta]^{\mathrm{T}}$, where x and y are, respectively, the abscissa and the ordinate of O' in $\mathcal{R}$ and ϑ is the angle $(\vec{x}, \vec{x}')$. The set of all the locations constitutes the *operational space of the platform*, denoted by $\mathcal{M}_p$.

The mobile platform wheels can be classified into four categories:

- the *fixed wheels* for which the axle has a fixed direction;
- the *steering wheels*, for which the orientation axis passes through the center of the wheel;

1. It is called as *posture* in Campion, Bastin, and D'Andréa-Novel (1996) but the choice of location allows us to use the same name for the robotic arms, the platforms and later for the mobile manipulators.

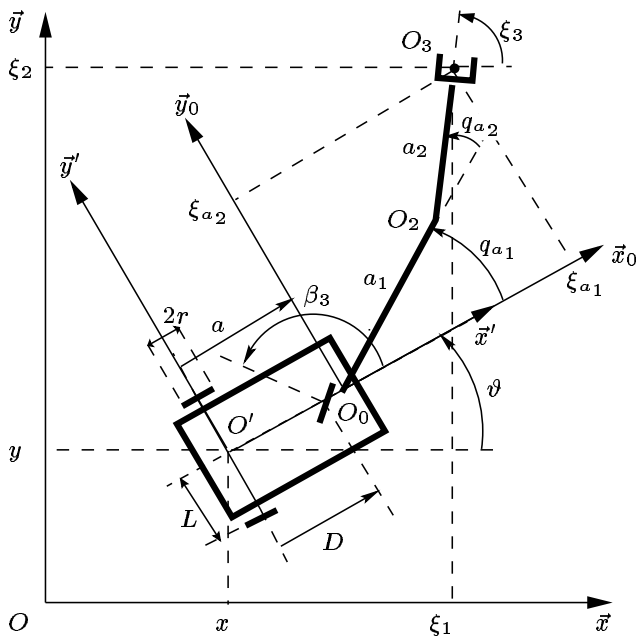

Fig. 1. Planar mobile manipulator with a car-like platform.

- the *castor wheels*, for which the orientation axis does not pass through the center of the wheel;
- the *Swedish wheels*, which are similar to the fixed wheels, with the exception of an additional parameter that describes the direction, with respect to the wheel plane, of the zero component of the velocity at the contact point.

It is assumed that the wheels always keep their shape, which is sensible in indoor robotics. We will consider that they all have the same radius, denoted by r.

Let $N = N_f + N_s + N_c + N_{sw}$ be the total number of wheels. N_f, N_s, N_c, and N_{sw} represent, respectively, the number of fixed, steering, castor and Swedish wheels. From now on, these indices correspond to the different types of wheels. Let $\boldsymbol{\varphi}_f$, $\boldsymbol{\varphi}_s$, $\boldsymbol{\varphi}_c$, and $\boldsymbol{\varphi}_{sw}$ be the vectors giving the rotation angles of the wheels about their horizontal axle; they all are variables. Let $\boldsymbol{\beta}_f$, $\boldsymbol{\beta}_s$, $\boldsymbol{\beta}_c$, and $\boldsymbol{\beta}_{sw}$ be the vectors giving the orientation of the wheels; $\boldsymbol{\beta}_f$ and $\boldsymbol{\beta}_{sw}$ are constants whereas $\boldsymbol{\beta}_s$ and $\boldsymbol{\beta}_c$ are variables. The N-dimensional rotation vector is $\boldsymbol{\varphi} = [\boldsymbol{\varphi}_f^{\mathrm{T}}\ \boldsymbol{\varphi}_s^{\mathrm{T}}\ \boldsymbol{\varphi}_c^{\mathrm{T}}\ \boldsymbol{\varphi}_{sw}^{\mathrm{T}}]^{\mathrm{T}}$. Then, the platform configuration is given by the n_p-dimensional vector, $\boldsymbol{q}_p = [\boldsymbol{\varphi}^{\mathrm{T}}\ \boldsymbol{\xi}_p^{\mathrm{T}}\ \boldsymbol{\beta}_s^{\mathrm{T}}\ \boldsymbol{\beta}_c^{\mathrm{T}}]^{\mathrm{T}}$, with $n_p = N + m_p + N_s + N_c \geqslant 3$.

2.1.2. Models

We assume that the conditions of r.w.s. of the wheels on the ground are always satisfied. Campion, Bastin, and D'Andréa-Novel (1996) show that there exists a systematic writing of the r.w.s. constraints.

By writing the r.w.s. constraints, we find out that there exist a vector, denoted by $\boldsymbol{\eta}_p$, that we call *control of mobility of the platform*, and a matrix $\Sigma(\boldsymbol{\beta}_s)$, which allow us to set the derivative of $\boldsymbol{\xi}_p$

$$\dot{\boldsymbol{\xi}}_p = R(\vartheta)\Sigma(\boldsymbol{\beta}_s)\boldsymbol{\eta}_p, \tag{1}$$

where

$$R(\vartheta) = \begin{bmatrix} C_\vartheta & -S_\vartheta & 0 \\ S_\vartheta & C_\vartheta & 0 \\ 0 & 0 & 1 \end{bmatrix},$$

with $C_\vartheta = \cos\vartheta$ and $S_\vartheta = \sin\vartheta$, is the rotation matrix expressing the orientation of $\mathcal{R}'$ with respect to $\mathcal{R}$. The model (1) relates the derivative of the platform location, in a given configuration, to its control of mobility. So it is called the IKLM *of the mobile platform*. The dimension δ_{m_p} of $\boldsymbol{\eta}_p$ is called the *degree of mobility of the platform*.

Additionally there exists an N_s-dimensional vector, denoted by $\boldsymbol{\zeta}_p$, that we call *control of steerability of the platform*, which represents the kinematic control of the steering wheels orientation:

$$\dot{\boldsymbol{\beta}}_s = \boldsymbol{\zeta}_p. \tag{2}$$

The dimension $\delta_{s_p} = N_s$ of $\boldsymbol{\zeta}_p$ is called the *degree of steerability of the platform*.

The *control (of maneuvrability) of the mobile platform* is then $\boldsymbol{u}_p = [\boldsymbol{\eta}_p^{\mathrm{T}}\ \boldsymbol{\zeta}_p^{\mathrm{T}}]^{\mathrm{T}}$. Its dimension, $\delta_{M_p} = \delta_{m_p} + \delta_{s_p}$, is called the *degree of maneuvrability of the platform*.

If we define $\boldsymbol{z}_p = [\boldsymbol{\xi}_p^{\mathrm{T}}\ \boldsymbol{\beta}_s^{\mathrm{T}}]^{\mathrm{T}}$, then

$$\dot{\boldsymbol{z}}_p = B_p(\vartheta,\ \boldsymbol{\beta}_s)\boldsymbol{u}_p,$$

with

$$B_p(\vartheta,\ \boldsymbol{\beta}_s) = \begin{bmatrix} R(\vartheta)\Sigma(\boldsymbol{\beta}_s) & 0 \\ 0 & I_{N_s} \end{bmatrix}.$$

where I_{N_s} is the N_s order identity matrix.

The r.w.s. constraints also allow us to set the derivative of $\boldsymbol{q}_p$

$$\dot{\boldsymbol{q}}_p = S_p(\vartheta,\ \boldsymbol{\beta}_s,\ \boldsymbol{\beta}_c)\boldsymbol{u}_p, \tag{3}$$

which relates the derivative of the platform configuration, in a given configuration, to its control (of maneuvrability). The corresponding model is called the *instantaneous kinematic configuration model* (IKCM) of the platform (Campion, Bastin, and D'Andréa-Novel 1996).

From now on, we assume that the mobile platform always has a number of actuators equal to its degree of maneuvrability.

2.1.3. Example

We consider the case of the car-like platform shown in Figure 2. The car is reduced to an equivalent vehicle (car-like platform) with only one steering wheel in the front, on the longitudinal axis of the vehicle,[2] and two fixed wheels on the same axle, in the back. The wheels are numbered in Figure 2. We denote by $\beta_3 = \beta_{s_1}$ the orientation of the steering wheel, by $\varphi_1 = \varphi_{f_1}$, $\varphi_2 = \varphi_{f_2}$, and $\varphi_3 = \varphi_{s_1}$ the rotation angles of the right fixed wheel, of the left fixed wheel and of the steering wheel, respectively (we hide indices $._f$ and $._s$ for simplicity). So we obtain $\boldsymbol{\varphi} = [\varphi_1\ \varphi_2\ \varphi_3]^{\mathrm{T}}$ and $\boldsymbol{q}_p = [\varphi_1\ \varphi_2\ \varphi_3\ x\ y\ \vartheta\ \beta_3]^{\mathrm{T}}$.

If we write the r.w.s. constraints, we obtain (Bayle 2001)

$$R^{\mathrm{T}}(\vartheta)\dot{\boldsymbol{\xi}}_p = \begin{bmatrix} -DS_{\beta_3} \\ 0 \\ C_{\beta_3} \end{bmatrix} \eta_p,$$

with $C_{\beta_3} = \cos\beta_3$ and $S_{\beta_3} = \sin\beta_3$. The control of mobility η_p is a scalar and then $\delta_{m_p} = 1$. The platform IKLM is thus

$$\dot{\boldsymbol{\xi}}_p = \begin{bmatrix} -DC_\vartheta S_{\beta_3} \\ -DS_\vartheta S_{\beta_3} \\ C_{\beta_3} \end{bmatrix} \eta_p. \tag{4}$$

As $\dot{\beta}_3 = \zeta_p$ (then $\delta_{m_p} = 1$), in this case, $\boldsymbol{u}_p = [\eta_p\ \zeta_p]^{\mathrm{T}}$ and then $\delta_{M_p} = 2$.

2. This model is convenient to describe the system equipped with two front wheels sharing the same instantaneous center of rotation.

The platform IKCM computation is detailed in Bayle (2001) (see Figure 2):

$$\dot{\boldsymbol{q}}_p = \begin{bmatrix} \dot{\boldsymbol{\varphi}} \\ \dot{\boldsymbol{\xi}}_p \\ \dot{\beta}_3 \end{bmatrix} = S_p(\vartheta,\ \beta_3)\boldsymbol{u}_p, \tag{5}$$

with

$$S_p(\vartheta,\ \beta_3) = \begin{bmatrix} \frac{1}{r}(DS_{\beta_3} - LC_{\beta_3}) & 0 \\ -\frac{1}{r}(DS_{\beta_3} + LC_{\beta_3}) & 0 \\ -\frac{D}{r} & 0 \\ -DC_\vartheta S_{\beta_3} & 0 \\ -DS_\vartheta S_{\beta_3} & 0 \\ C_{\beta_3} & 0 \\ 0 & 1 \end{bmatrix}.$$

2.2. Robotic Arm Case

2.2.1. Description

We consider a robotic arm built from n_a mobile bodies (supposed perfectly rigid) articulated by n_a revolute and/or prismatic joints. The most usual way to model a robotic arm consists of using the Denavit–Hartenberg modified parameters (Craig 1989; Khalil and Kleinfinger 1986). We associate the frame $\mathcal{R}_i = (O_i,\ \vec{x}_i,\ \vec{y}_i,\ \vec{z}_i)$, with $i = 0,\ 1,\ \ldots,\ n_a$, to the ith body of the robotic arm. So, the frame $\mathcal{R}_0$ is linked to the base. The center of the EE (tool or grip) is denoted by O_{n_a+1}. So, both points O_{n_a} and O_{n_a+1} are linked to the EE. The Denavit–Hartenberg modified parameters define the *location* (position and orientation) of all the bodies of the robotic arm, i.e., its whole geometry.

The *robotic arm configuration* is known when the position of all its points in $\mathcal{R}_0$ are known (Neimark and Fufaev 1972). It is defined by a vector $\boldsymbol{q}_a$ of n_a independent coordinates. These coordinates, called *generalized coordinates of the robotic arm*, characterize the values of the different joints: rotation angles for the revolute ones, translations for the prismatic joints. The configuration $\boldsymbol{q}_a = [q_{a_1}\ q_{a_2}\ \ldots\ q_{a_{n_a}}]^{\mathrm{T}}$ is an element of the *configuration space* of the robotic arm, denoted by $\mathcal{N}_a$.

The *location of the robotic arm EE* is given by an m_a-dimensional vector, denoted by $\boldsymbol{\xi}_a = [\xi_{a_1}\ \xi_{a_2}\ \ldots\ \xi_{a_{m_a}}]^{\mathrm{T}}$. Its m_a coordinates are the *operational coordinates of the robotic arm*. They define the position and the orientation of the EE in $\mathcal{R}_0$. The set of the locations constitutes the *operational space of the robotic arm*, denoted by $\mathcal{M}_a$. We define: (i) the position of the EE in $\mathcal{R}_0$ by the Cartesian coordinates of O_{n_a+1}, which is the most usual choice, $[\xi_{a_1}\ \xi_{a_2}\ \xi_{a_3}]^{\mathrm{T}}$; (ii) the orientation of the EE with the Euler classical angles (Paul 1981), $[\xi_{a_4}\ \xi_{a_5}\ \xi_{a_6}]^{\mathrm{T}} = [\psi\ \theta\ \varphi]^{\mathrm{T}}$. This choice is particularly relevant in this study (see Section 2.3).

REMARK. The location of the robotic arm EE can be defined in different ways according to the task to achieve. So, for a

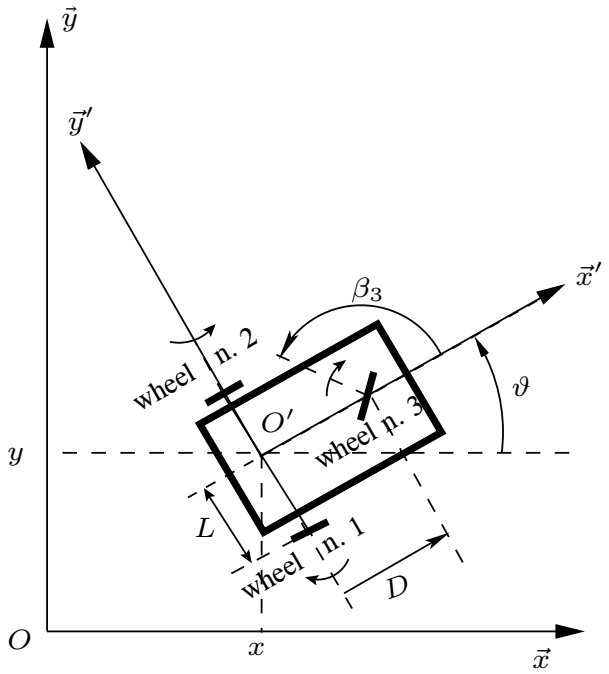

Fig. 2. The car-like mobile platform.

planar problem, we will consider only the EE position and orientation in the plane. Also, we can consider only the planar position of the EE, as in the coming example.

2.2.2. Models

The *kinematic model* (KM) of a robotic arm sets the location of its EE as a function of its configuration (or its operational coordinates as functions of its generalized coordinates):

$$\begin{array}{rccl} \boldsymbol{f}_a: & \mathcal{N}_a & \longrightarrow & \mathcal{M}_a \\ & \boldsymbol{q}_a & \longmapsto & \boldsymbol{\xi}_a = \boldsymbol{f}_a(\boldsymbol{q}_a). \end{array}$$

The *instantaneous kinematic model* (IKM) of a robotic arm sets the derivative of its location as a function of the derivative of its configuration (or its *operational velocities* as functions of its *generalized velocities*):

$$\begin{array}{rccl} J_a(\boldsymbol{q}_a): & T_{\boldsymbol{q}_a}\mathcal{N}_a & \longrightarrow & T_{\boldsymbol{\xi}_a}\mathcal{M}_a \\ & \dot{\boldsymbol{q}}_a & \longmapsto & \dot{\boldsymbol{\xi}}_a = J_a(\boldsymbol{q}_a)\dot{\boldsymbol{q}}_a. \end{array}$$

It uses the Jacobian matrix $J_a(\boldsymbol{q}_a)$ of the function $\boldsymbol{f}_a$: $J_a(\boldsymbol{q}_a) = \frac{\partial \boldsymbol{f}_a}{\partial \boldsymbol{q}_a}$. The configurations such that the rank of $J_a(\boldsymbol{q}_a)$ decreases are singular kinematic configurations and the problem, robotic arm and task, is redundant when $n_a > m_a$.

We define the *vector of the kinematic control of the robotic arm* by

$$\boldsymbol{u}_a = \dot{\boldsymbol{q}}_a. \tag{6}$$

We do not evoke the other models of the robotic arms. For further precision, we will refer to general robotics books, for example Craig (1989) or Sciavicco and Siciliano (2000).

2.2.3. Example

These concepts are easy to illustrate on the robotic arm of the mobile manipulator shown in Figure 3 (see Figure 1). This robotic arm is built from two bodies (the lengths of which are, respectively, a_1 and a_2), articulated by two revolute joints with vertical parallel axes. O_0 is linked to the base of this robotic arm and O_3 to the center of the EE. The robotic arm configuration is given by the rotation angles q_{a_1} and q_{a_2} and so $\boldsymbol{q}_a = [q_{a_1}\ q_{a_2}]^{\mathrm{T}}$. It is not possible to take into account both the position and orientation of the EE, since $m_a = 3 > n_a$. Consequently, we define the EE location only by the planar position of O_3 in $\mathcal{R}_0$: $\boldsymbol{\xi}_a = [\xi_{a_1}\ \xi_{a_2}]^{\mathrm{T}}$. Therefore, the operational space $\mathcal{M}_a$ is two-dimensional.

The robotic arm KM is

$$\begin{array}{rcl} \xi_{a_1} & = & a_1 C_1 + a_2 C_{12}, \\ \xi_{a_2} & = & a_1 S_1 + a_2 S_{12}, \end{array} \tag{7}$$

where $C_i = \cos q_{ai}$, $S_i = \sin q_{ai}$, $C_{ij} = \cos(q_{ai} + q_{aj})$ and $S_{ij} = \sin(q_{ai} + q_{aj})$, $\forall i,\ j = 1,\ 2$. Thus, the IKM is $\dot{\boldsymbol{\xi}}_a = J_a(\boldsymbol{q}_a)\dot{\boldsymbol{q}}_a$, with

$$J_a(\boldsymbol{q}_a) = \begin{bmatrix} -(a_1 S_1 + a_2 S_{12}) & -a_2 S_{12} \\ a_1 C_1 + a_2 C_{12} & a_2 C_{12} \end{bmatrix}.$$

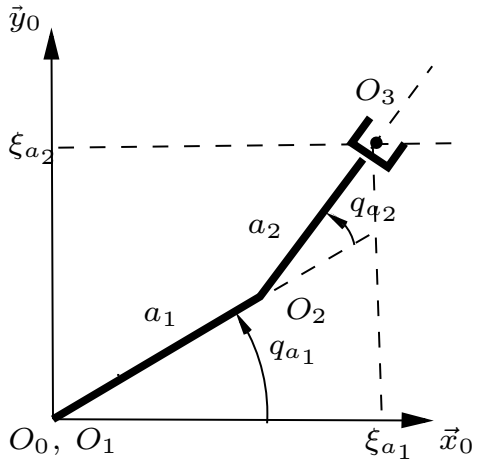

Fig. 3. A planar robotic arm with two revolute joints.

2.3. Mobile Manipulator Case

2.3.1. Description

We consider the general case of a mobile manipulator built from a mobile platform equipped with an on-board robotic arm, introduced respectively in Sections 2.1 and 2.2. The coordinates of O_0 in $\mathcal{R}'$ are given by $[a\ b\ 0]^{\mathrm{T}}$ (see Figure 4).

The *mobile manipulator configuration* is known when the position of all its points in $\mathcal{R}$ are known (Neimark and Fufaev 1972). It is defined by a vector $\boldsymbol{q}$ of n independent coordinates, called *generalized coordinates of the mobile manipulator*. We can choose $\boldsymbol{q} = [q_1\ q_2\ \ldots\ q_n]^{\mathrm{T}} = [\boldsymbol{q}_a^{\mathrm{T}}\ \boldsymbol{q}_p^{\mathrm{T}}]^{\mathrm{T}}$. We notice that $n = n_a + n_p$, where n_a and n_p are, respectively, the dimensions of the generalized spaces associated with the robotic arm and the platform. The configuration $\boldsymbol{q}$ is an element of the *configuration space* of the mobile manipulator, denoted by $\mathcal{N}$.

The *location of the mobile manipulator EE* is given by the m-dimensional vector $\boldsymbol{\xi} = [\xi_1\ \xi_2\ \ldots\ \xi_m]^{\mathrm{T}}$. Its m coordinates are *operational coordinates of the mobile manipulator*. They define the position and the orientation of the EE in $\mathcal{R}$. The set of all the locations constitutes the *operational space of the mobile manipulator*, denoted by $\mathcal{M}$. We define: (i) the position of the EE in $\mathcal{R}$ by the Cartesian coordinates of O_{n_a+1}, $[\xi_1\ \xi_2\ \xi_3]^{\mathrm{T}}$; (ii) the orientation of the EE with the Euler classical angles (Paul 1981), $[\xi_4\ \xi_5\ \xi_6]^{\mathrm{T}} = [\beta\ \theta\ \varphi]^{\mathrm{T}}$. Note that $\xi_5 = \xi_{a_5}$ and $\xi_6 = \xi_{a_6}$. This property justifies the choice of the Euler classical angles.

REMARKS. The remark in Section 2.2.1 is still relevant; the location of the mobile manipulator EE can be defined in different ways according to the task to achieve, as in the example in Section 2.3.3, in which we only consider the planar position of the EE.

2.3.2. Models

The KM *of a mobile manipulator* sets the location of its EE as a function of the robotic arm configuration and of the platform location (or its operational coordinates as functions of the robotic arm generalized coordinates and of the mobile platform operational coordinates):

$$\begin{array}{rccl} \boldsymbol{f}: & \mathcal{N}_a \times \mathcal{M}_p & \longrightarrow & \mathcal{M} \\ & (\boldsymbol{q}_a,\ \boldsymbol{\xi}_p) & \longmapsto & \boldsymbol{\xi} = \boldsymbol{f}(\boldsymbol{q}_a,\ \boldsymbol{\xi}_p). \end{array}$$

The shape of the mobile manipulators we are studying is shown in Figure 4, regardless of the type of wheels. For any wheeled mobile platform with location $\boldsymbol{\xi}_p = [x\ y\ \vartheta]^{\mathrm{T}}$ equipped with a robotic arm with configuration $\boldsymbol{q}_a$ and location $\boldsymbol{\xi}_a$, the position of the mobile manipulator EE in $\mathcal{R}$ is

$$\begin{array}{rcl} \xi_1 &=& x + (a + \xi_{a_1})C_\vartheta - (b + \xi_{a_2})S_\vartheta \\ \xi_2 &=& y + (a + \xi_{a_1})S_\vartheta + (b + \xi_{a_2})C_\vartheta \\ \xi_3 &=& \xi_{a_3} \end{array} \tag{8}$$

and its orientation is

$$\begin{array}{rcl} \xi_4 &=& \beta = \vartheta + \psi \\ \xi_5 &=& \theta \\ \xi_6 &=& \varphi. \end{array} \tag{9}$$

The IKM *of a mobile manipulator* sets the derivative of its location as a function of the derivatives of the robotic arm configuration and of the location of the mobile platform (or its operational velocities as functions of the robotic arm generalized velocities and of the mobile platform operational velocities):

$$\dot{\boldsymbol{\xi}} = \frac{\partial \boldsymbol{f}}{\partial \boldsymbol{q}_a}(\boldsymbol{q}_a,\ \vartheta)\,\dot{\boldsymbol{q}}_a + \frac{\partial \boldsymbol{f}}{\partial \boldsymbol{\xi}_p}(\boldsymbol{q}_a,\ \vartheta)\,\dot{\boldsymbol{\xi}}_p. \tag{10}$$

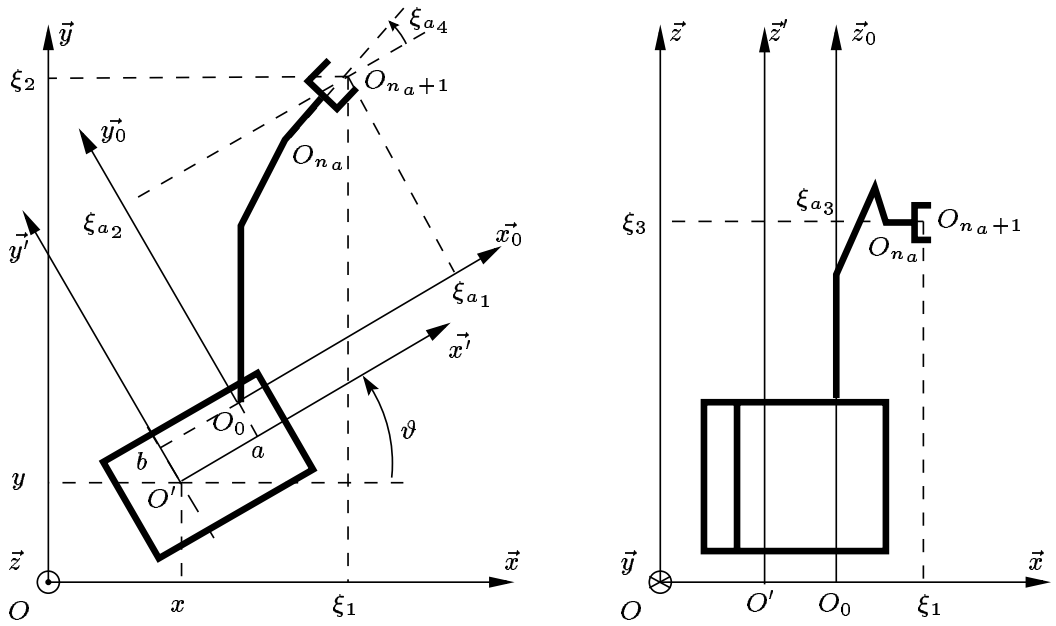

Fig. 4. Geometry of mobile manipulators.

Note that $\boldsymbol{f}$ is a function of $\boldsymbol{q}_a$ and $\boldsymbol{\xi}_p$, whereas its partial derivatives only depend on $\boldsymbol{q}_a$ and ϑ. From eqs. (8) and (9)

$$\frac{\partial \boldsymbol{f}}{\partial \boldsymbol{q}_a}(\boldsymbol{q}_a,\ \vartheta) = \begin{bmatrix} J_{a_{1,\star}} C_\vartheta - J_{a_{2,\star}} S_\vartheta \\ J_{a_{1,\star}} S_\vartheta + J_{a_{2,\star}} C_\vartheta \\ J_{a_{3,\star}} \\ J_{a_{4,\star}} \\ J_{a_{5,\star}} \\ J_{a_{6,\star}} \end{bmatrix},$$

where $J_{a_{k,\star}}$ is the kth line of the robotic arm Jacobian matrix and

$$\frac{\partial \boldsymbol{f}}{\partial \boldsymbol{\xi}_p}(\boldsymbol{q}_a,\ \vartheta) = \begin{bmatrix} 1 & 0 & -((a+\xi_{a_1})S_\vartheta + (b+\xi_{a_2})C_\vartheta) \\ 0 & 1 & (a+\xi_{a_1})C_\vartheta - (b+\xi_{a_2})S_\vartheta \\ 0 & 0 & 0 \\ 0 & 0 & 1 \\ 0 & 0 & 0 \\ 0 & 0 & 0 \end{bmatrix}.$$

We define the control of mobility of the mobile manipulator by $\boldsymbol{\eta} = [\boldsymbol{u}_a^{\mathrm{T}}\ \boldsymbol{\eta}_p^{\mathrm{T}}]^{\mathrm{T}}$. Its dimension $\delta_m = n_a + \delta_{m_p}$ is called the *degree of mobility of the mobile manipulator*. The IKLM *of a mobile manipulator* sets the derivative of its location as a function of its control of mobility. According to eqs. (1) and (6), eq. (10) is written as

$$\dot{\boldsymbol{\xi}} = \frac{\partial \boldsymbol{f}}{\partial \boldsymbol{q}_a}(\boldsymbol{q}_a,\ \vartheta)\boldsymbol{u}_a + \frac{\partial \boldsymbol{f}}{\partial \boldsymbol{\xi}_p}(\boldsymbol{q}_a,\ \vartheta)R(\vartheta)\Sigma(\boldsymbol{\beta}_s)\boldsymbol{\eta}_p.$$

So the IKLM is written as

$$\dot{\boldsymbol{\xi}} = \bar{J}(\boldsymbol{q}_a,\ \vartheta,\ \boldsymbol{\beta}_s)\boldsymbol{\eta}, \tag{11}$$

with $\bar{J}(\boldsymbol{q}_a,\ \vartheta,\ \boldsymbol{\beta}_s) = \left[\frac{\partial \boldsymbol{f}}{\partial \boldsymbol{q}_a}(\boldsymbol{q}_a,\ \vartheta) \quad \frac{\partial \boldsymbol{f}}{\partial \boldsymbol{\xi}_p}(\boldsymbol{q}_a,\ \vartheta)R(\vartheta)\Sigma(\boldsymbol{\beta}_s)\right]$ being an $m \times \delta_m$ matrix.

The configurations such that the rank of $\bar{J}(\boldsymbol{q}_a,\ \vartheta,\ \boldsymbol{\beta}_s)$ decreases are singular kinematic configurations and the problem, mobile manipulator and task, is redundant when $\delta_m > m$.

We notice that the derivative of the mobile manipulator EE location does not depend on the derivative of the steering wheels orientation, *for a given configuration*, i.e., does not depend on the control of steerability $\boldsymbol{\zeta}_p$ of the platform.

We define the *control (of maneuvrability) of the mobile manipulator* by $\boldsymbol{u} = [\boldsymbol{u}_a^{\mathrm{T}}\ \boldsymbol{u}_p^{\mathrm{T}}]^{\mathrm{T}}$ i.e., $\boldsymbol{u} = [\dot{\boldsymbol{q}}_a^{\mathrm{T}}\ \boldsymbol{\eta}_p^{\mathrm{T}}\ \boldsymbol{\zeta}_p^{\mathrm{T}}]^{\mathrm{T}}$. Its dimension, $\delta_M = n_a + \delta_{M_p} = \delta_m + \delta_{s_p}$ is called the *degree of maneuvrability of the mobile manipulator*. If we define $\boldsymbol{z} = [\boldsymbol{\xi}^{\mathrm{T}}\ \boldsymbol{\beta}_s^{\mathrm{T}}]^{\mathrm{T}}$, from eqs. (11) and (2), we obtain

$$\dot{\boldsymbol{z}} = B(\boldsymbol{q}_a,\ \vartheta,\ \boldsymbol{\beta}_s)\boldsymbol{u},$$

with

$$B(\boldsymbol{q}_a,\ \vartheta,\ \boldsymbol{\beta}_s) = \begin{bmatrix} \bar{J}(\boldsymbol{q}_a,\ \vartheta,\ \boldsymbol{\beta}_s) & 0 \\ 0 & I_{N_s} \end{bmatrix}.$$

We also define the IKCM of the mobile manipulator by analogy with the case of the mobile platforms. When the platform IKCM is known, from eq. (3) we write

$$\dot{\boldsymbol{q}} = S(\vartheta,\ \boldsymbol{\beta}_s,\ \boldsymbol{\beta}_c)\boldsymbol{u}, \tag{12}$$

where

$$S(\vartheta,\ \boldsymbol{\beta}_s,\ \boldsymbol{\beta}_c) = \begin{bmatrix} I_{n_a} & 0 \\ 0 & S_p(\vartheta,\ \boldsymbol{\beta}_s,\ \boldsymbol{\beta}_c) \end{bmatrix}.$$

It is fundamental to notice that, in general, the dimension of operational space m is less than the degree of mobility δ_m of the mobile manipulator. In this case, we recall that the problem, mobile manipulator and task, is redundant.

2.3.3. Example

We consider the mobile manipulator shown in Figure 1, where $b = 0$ for the sake of simplicity. Again, we reduce the location to the planar position of the EE in the horizontal plane. The position O_3 in the frame $\mathcal{R}$ is thus given by its Cartesian coordinates ξ_1 and ξ_2. The configuration is $\boldsymbol{q} = [q_{a_1}\ q_{a_2}\ \varphi_1\ \varphi_2\ \varphi_3\ x\ y\ \vartheta\ \beta_3]^{\mathrm{T}}$. The control of maneuvrability of the mobile manipulator is $\boldsymbol{u} = [\boldsymbol{u}_a^{\mathrm{T}}\ \boldsymbol{u}_p^{\mathrm{T}}]^{\mathrm{T}} = [\dot{q}_{a_1}\ \dot{q}_{a_2}\ \eta_p\ \zeta_p]^{\mathrm{T}}$. The degree of mobility of the mobile manipulator is $\delta_m = n_a + \delta_{m_p} = 2 + 1 = 3$. Its degree of maneuvrability is $\delta_M = n_a + \delta_{M_p} = 2 + 2 = 4$ or $\delta_M = \delta_m + \delta_{s_p} = 3 + 1 = 4$.

According to eqs. (7) and (8), the KM of this mobile manipulator is

$$\begin{aligned} \xi_1 &= x + (a + a_1C_1 + a_2C_{12})C_\vartheta - (a_1S_1 + a_2S_{12})S_\vartheta, \\ \xi_2 &= y + (a + a_1C_1 + a_2C_{12})S_\vartheta + (a_1S_1 + a_2S_{12})C_\vartheta. \end{aligned} \tag{13}$$

Using eqs. (4), (11) and (13), we obtain

$$\dot{\boldsymbol{\xi}} = \begin{bmatrix} \dot{\xi}_1 \\ \dot{\xi}_2 \end{bmatrix} = \bar{J}(q_{a_1},\ q_{a_2},\ \vartheta,\ \beta_3) \begin{bmatrix} \dot{q}_{a_1} \\ \dot{q}_{a_2} \\ \eta_p \end{bmatrix},$$

where

$$\bar{J}(q_{a_1},\ q_{a_2},\ \vartheta,\ \beta_3) = \begin{bmatrix} D_2 & D_1 & D_4 \\ D_6 & D_5 & D_7 \end{bmatrix},$$

with the following intermediate variables:

$$\begin{aligned} C_{\vartheta 1} &= \cos(\vartheta + q_{a_1}), \\ S_{\vartheta 1} &= \sin(\vartheta + q_{a_1}), \\ C_{\vartheta 12} &= \cos(\vartheta + q_{a_1} + q_{a_2}), \\ S_{\vartheta 12} &= \sin(\vartheta + q_{a_1} + q_{a_2}), \\ D_1 &= -a_2S_{\vartheta 12}, \\ D_2 &= -a_1S_{\vartheta 1} + D_1, \\ D_3 &= -DS_{\beta_3}, \\ D_4 &= C_\vartheta D_3 + C_{\beta_3}(D_2 - aS_\vartheta), \\ D_5 &= a_2C_{\vartheta 12}, \\ D_6 &= a_1C_{\vartheta 1} + D_5, \\ D_7 &= S_\vartheta D_3 + C_{\beta_3}(D_6 + aC_\vartheta). \end{aligned}$$

If we take into account eqs. (2) and (13), we also obtain

$$\dot{\boldsymbol{z}} = \begin{bmatrix} \dot{\xi}_1 \\ \dot{\xi}_2 \\ \dot{\beta}_3 \end{bmatrix} = B(q_{a_1},\ q_{a_2},\ \vartheta,\ \beta_3) \begin{bmatrix} \dot{q}_{a_1} \\ \dot{q}_{a_2} \\ \eta_p \\ \zeta_p \end{bmatrix},$$

with $B(q_{a_1},\ q_{a_2},\ \vartheta,\ \beta_3) = \begin{bmatrix} \bar{J}(q_{a_1},\ q_{a_2},\ \vartheta,\ \beta_3) & 0 \\ 0 & 1 \end{bmatrix}$.

The IKCM of the mobile manipulator $\dot{\boldsymbol{q}} = [\dot{q}_{a_1}\ \dot{q}_{a_2}\ \dot{\varphi}_1\ \dot{\varphi}_2\ \dot{\varphi}_3\ \dot{x}\ \dot{y}\ \dot{\vartheta}\ \dot{\beta}_3]^{\mathrm{T}} = S(\vartheta,\ \beta_3)[\dot{q}_{a_1}\ \dot{q}_{a_2}\ \eta_p\ \zeta_p]^{\mathrm{T}}$ is immediately obtained using the platform IKCM (5):

$$S(\vartheta,\ \beta_3) = \begin{bmatrix} 1 & 0 & 0 & 0 \\ 0 & 1 & 0 & 0 \\ 0 & 0 & \frac{1}{r}(DS_{\beta_3} - lC_{\beta_3}) & 0 \\ 0 & 0 & -\frac{1}{r}(DS_{\beta_3} + lC_{\beta_3}) & 0 \\ 0 & 0 & -\frac{D}{r} & 0 \\ 0 & 0 & -DC_\vartheta S_{\beta_3} & 0 \\ 0 & 0 & -DS_\vartheta S_{\beta_3} & 0 \\ 0 & 0 & C_{\beta_3} & 0 \\ 0 & 0 & 0 & 1 \end{bmatrix}.$$

For other examples, we refer to Bayle (2001).

3. Manipulability

3.1. The Manipulability of Robotic Arms

In this section we introduce elements of the manipulability theory as developed by Yoshikawa. For more precision, the reader may refer to Yoshikawa (1990) or Bayle, Fourquet, and Renaud (2001b).

Let us consider a robotic arm and its IKM $\dot{\boldsymbol{\xi}}_a = J_a(\boldsymbol{q}_a)\dot{\boldsymbol{q}}_a$. For a given configuration $\boldsymbol{q}_a$, manipulability characterizes the subset of the realizable velocities $\dot{\boldsymbol{\xi}}_a$ such that the corresponding joint velocity verifies $||\dot{\boldsymbol{q}}_a|| \leq 1$.

Let $J_a(\boldsymbol{q}_a) = U_a(\boldsymbol{q}_a)\Sigma_a(\boldsymbol{q}_a)V_a^T(\boldsymbol{q}_a)$ be the singular value decomposition (SVD) of matrix $J_a(\boldsymbol{q}_a)$ (Golub and Van Loan 1996). $U_a(\boldsymbol{q}_a)$ and $V_a(\boldsymbol{q}_a)$ are orthogonal and $\Sigma_a(\boldsymbol{q}_a)$ has the ordered singular values on its diagonal. Let us assume that $U_a(\boldsymbol{q}_a) = [\boldsymbol{U}_{a1}\ \boldsymbol{U}_{a2}\ \ldots\ \boldsymbol{U}_{am_a}]$ and that the singular values are $\sigma_1 \geq \sigma_2 \geq \ldots \geq \sigma_{m_a}$.

Then the set of realizable velocities $\dot{\boldsymbol{\xi}}_a$, such that the corresponding joint velocity verifies $||\dot{\boldsymbol{q}}_a|| \leq 1$, is given by

$$\sum_{\sigma_i \neq 0} \left(\frac{(\dot{\boldsymbol{\Xi}}_a)_i}{\sigma_i} \right)^2 \leq 1,$$

with $\dot{\boldsymbol{\Xi}}_a = U_a(\boldsymbol{q}_a)^{\mathrm{T}}\dot{\boldsymbol{\xi}}_a$. This is the equation of an m-dimensional ellipsoid with the main axis given by the $\boldsymbol{U}_{ai}$, $i = 1, 2, \ldots, m_a$ of associated radii σ_i. Its volume is proportional to the product $\sigma_1\sigma_2 \ldots \sigma_{m_a}$.

Thanks to these theoretical bases we can analyze the instantaneous kinematics of a robotic arm from different points of view. The visualization of the ellipsoid may be interesting but of course it only applies when the operational space is two-dimensional or three-dimensional. So, we often consider only positioning of the EE. The shape of the manipulability ellipsoid, gives information on the capabilities of the arm to move in the different directions of the operational space.

Additionally, we can define different algebraic measures to characterize this ellipsoid. They are often called *manipulability measures* and give a scalar information. The more usual manipulability measure is $w_a = \sigma_1\sigma_2 \ldots \sigma_{m_a}$ which is proportional to the ellipsoid volume. It thus gives quantitative information on the manipulability. Moreover, it can be shown that $w_a = \sqrt{\det(J_a(\boldsymbol{q}_a)J_a^T(\boldsymbol{q}_a))}$, which simplifies into $w_a = |\det J_a(\boldsymbol{q}_a)|$ when $J_a(\boldsymbol{q}_a)$ is square; it is not necessary to apply the SVD to compute w_a.

If we look for more qualitative information, we can compute the ratio of the minimum to the maximum radii of the ellipsoid: $w_{a_2} = \frac{\sigma_{m_a}}{\sigma_1}$. Yoshikawa underlines that it is the reciprocal of the *condition number* (numerical information to evaluate the distance to singularities) of the Jacobian $J_a(\boldsymbol{q}_a)$, which is an interesting computational feature. In this paper, we define a manipulability measure[3] extending the notion of *eccentricity* of the ellipse:

$$w_{a_5} = \sqrt{1 - \frac{\sigma_{m_a}^2}{\sigma_1^2}}.$$

This measure is related to the shape of the ellipsoids, and thus to the ability of the EE to move in privileged directions of the operational space. For instance, in a planar case, if $w_{a_5} = 0$, the ellipse is a circle and if $w_{a_5} = 1$ it is flat, which means that the EE can only move in one direction (it is closely related to w_{a_2} and thus to the condition number).

EXAMPLE. If we consider only the arm of our planar mobile manipulator for a planar positioning task, we can illustrate the different previous items. We could represent the manipulability ellipses of this arm all around its workspace. Rather, we examine the evolution of manipulability when the EE position follows a straight line along the abscissa axis from a folded configuration ($q_{a_1} = \frac{\pi}{2}, q_{a_2} = -\frac{\pi}{2}$) to a totally extended one ($q_{a_1} = q_{a_2} = 0$). Figure 5 displays the manipulability measure w_{a_5} based on the ellipses eccentricity, as a function of the arm extent, similar to Yoshikawa (1990) (see also Extension 1). It gives information on the shape of the ellipses. Indeed, as w_{a_5} decreases, the possible EE velocities become more isotropic ($w_{a_5} = 0$ would mean that the EE can move equally in any direction with a bounded velocity control vector).

We notice that, in the case of the robotic arm, there is a singularity when $\boldsymbol{q}_a = [0\ 0]^{\mathrm{T}}$. Indeed $\det J_a(\boldsymbol{q}_a) = 0$ in this configuration, which implies $w_a = 0$, and thus $\sigma_{m_a} = 0$, which implies $w_{a_5} = 1$. In Figure 5, it corresponds to a degenerated ellipse.

3.2. The Manipulability of Mobile Manipulators

We now take into account the mobile platform. The first contribution, to our knowledge, that dealt with manipulability in mobile manipulation is devoted to the manipulability of the sole arm (Yamamoto and Yun 1994). Depending on the tasks at hand, there is an interest in considering the ability of generating velocities at the EE by acting on the robotic arm or by acting on the whole system. Here, we develop an analysis of the whole mobile manipulator manipulability.

We now wish to establish a similar analysis when the robotic arm is mounted on a wheeled mobile platform. The results recalled in Section 3.1, in the case of a robotic arm, use the IKM. A similar framework can be used for nonholonomic mobile manipulators from the definition of the IKLM, given by eq. (11)

$$\dot{\boldsymbol{\xi}} = \bar{J}(\boldsymbol{q}_a,\ \vartheta,\ \boldsymbol{\beta}_s)\boldsymbol{\eta},$$

since this model describes the instantaneous velocities of the EE for given controls of mobility. Thus, the results of Section 3.1 can be rewritten by replacing, respectively, $\boldsymbol{\xi}_a, \boldsymbol{u}_a$, and $J_a(\boldsymbol{q}_a)$ by $\boldsymbol{\xi}, \boldsymbol{\eta}$, and $\bar{J}(\boldsymbol{q}_a,\ \vartheta,\ \boldsymbol{\beta}_s)$. In this way, we are looking for the realizable EE velocities such that the corresponding control of mobility $\boldsymbol{\eta}$ verifies $||\boldsymbol{\eta}||^2 \leqslant 1$. If we consider eq. (11) and that we set

$$B_1(\boldsymbol{q}_a,\ \vartheta,\ \boldsymbol{\beta}_s) = \left[\bar{J}(\boldsymbol{q}_a,\ \vartheta,\ \boldsymbol{\beta}_s) \quad 0\right],$$

then

$$\dot{\boldsymbol{\xi}} = B_1(\boldsymbol{q}_a,\ \vartheta,\ \boldsymbol{\beta}_s)\boldsymbol{u}.$$

REMARKS.

- It is easy to show that the condition $||\boldsymbol{u}||^2 \leqslant 1$ would lead to the same ellipsoid of manipulability in operational space as the condition $||\boldsymbol{\eta}||^2 \leqslant 1$. In fact, the control of steerability has no effect on instantaneous velocity of the EE or, in other words, the SVDs of $\bar{J}(\boldsymbol{q}_a,\ \vartheta,\ \boldsymbol{\beta}_s)$ and of $B_1(\boldsymbol{q}_a,\ \vartheta,\ \boldsymbol{\beta}_s)$ lead to the same singular values and to the same main axis. Indeed, let $A = U\Sigma V^{\mathrm{T}}$ be the SVD of matrix A, then the SVD of matrix $A' = [A\ 0]$ is

  $$A' = U[\Sigma\ 0]\begin{bmatrix} V^{\mathrm{T}} \\ 0 \end{bmatrix}.$$

  It is generally not possible to separate analytically the effects of the platform and of the robotic arm on manipulability. So they will be visualized through several numeric simulations.

- It is generally desirable to normalize (Yoshikawa 1990) the ellipsoids of manipulability to take into account the nature of the joints (rotations/translations). For instance, we can use the maximum generalized velocities to normalize the manipulability ellipsoids (Yamamoto and Yun 1999). It may also be important to take into account the differences between the subsystems, from a dynamic point of view. To do so, we can modify

3. We call this measure w_{a_5} as Yoshikawa defines four other measures.

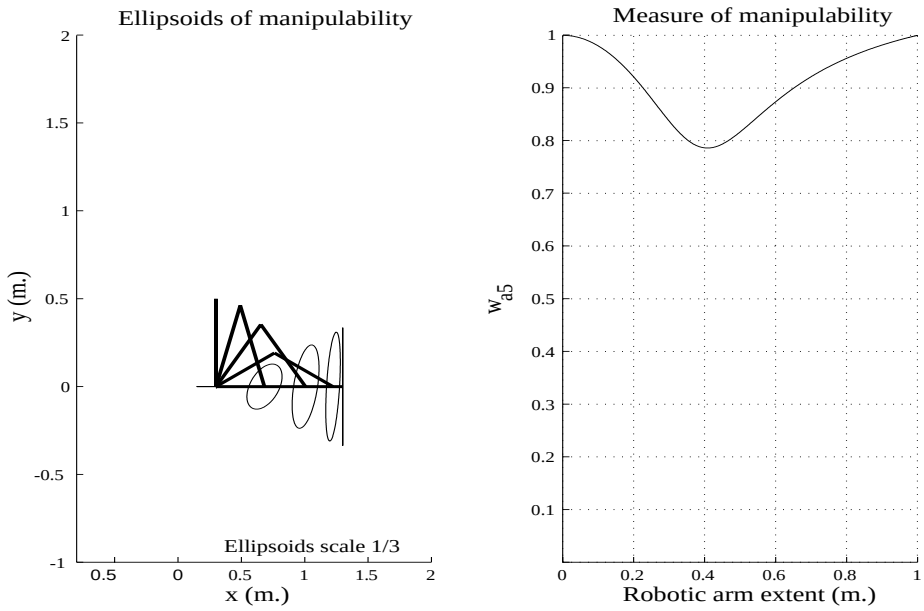

Fig. 5. Manipulability analysis for the robotic arm.

the manipulability definition, for instance by weighting $\bar{J}(\boldsymbol{q}_a,\ \vartheta,\ \boldsymbol{\beta}_s)$ with the kinetic energy matrix (Lipkin and Duffy 1988). This assumes that this matrix is known, or estimated.

We use the maximum generalized velocities to normalize the manipulability ellipsoids in our simulations, but for the sake of simplicity we do not mention it in the text.

- Errors in the estimation of the robot localization are among the key problems in mobile robotics. Concerning the analysis of manipulability of the mobile manipulator, the uncertainty on the mobile platform localization also has an influence. Indeed, the computation of $\bar{J}(\boldsymbol{q}_a,\ \vartheta,\ \boldsymbol{\beta}_s)$ requires the knowledge of the orientation of the platform in the reference frame. In the case of an important drift on the estimation of this value, the manipulability measure is necessarily affected.

EXAMPLES. We consider the case of the mobile manipulator in Figure 1, modeled in Section 2.3. We choose $a = 0.8$ m, $b = 0$. The next two simulations are done with the configurations of the robotic arm used in Section 3.1. Manipulability measures for the mobile manipulator are derived from the previous observations and denoted by w and w_5.

First, the steering wheel plane is parallel to the longitudinal axis of the platform, i.e., $\beta_3 = \frac{\pi}{2}$ (see Figure 2). Figure 6 shows the evolutions of the manipulability ellipsoids and of the measure of manipulability w_5, as functions of the robotic arm stretching (see also Extension 2).

The effects of associating a mobile platform and a robotic arm are significant concerning the manipulability. A comparison of Figures 5 and 6 clearly brings to light the contribution of the mobile platform to the manipulability of the whole system. Particularly, we notice that the ellipsoid of manipulability no longer vanishes when q_{a_1}, q_{a_2} and ϑ are zero. In this configuration, $w_5 \neq 1$, compared to $w_{a_5} = 1$ for the robotic arm. So, the mobile manipulator configuration is no longer singular. Nevertheless, the configuration corresponding to $q_{a_1} = \frac{\pi}{2}$ and $q_{a_2} = -\frac{\pi}{2}$ is still singular.

As first noticed by Yamamoto and Yun (1999), manipulability also shows the constraints acting on the system. As the platform is nonholonomic, its influence on manipulability is not the same in all the directions of the operational space. This appears in Figure 7; in this simulation, we modify the mobile manipulator configuration by rotating the vertical axis of the steering wheel of the platform (see also Extension 3). It is placed so that its plane becomes perpendicular to the longitudinal axis of the platform, i.e., $\beta_3 = 0$ (see Figure 2). The locations of the EE are still the same as in the previous examples. We then visualize the evolution of the ellipsoids of manipulability and of the measure w_5, as functions of the arm extent.

The steering wheel orientation creates a constraint on the system, which cannot roll without slipping along the longitudinal axis of the platform. So, when the robotic arm is completely stretched, the EE can only move in the direction perpendicular to this axis; it corresponds to a measure of manipulability $w_5 = 1$ and also to $\bar{J}(\boldsymbol{q}_a,\ \vartheta,\ \boldsymbol{\beta}_s)$ rank deficiency.

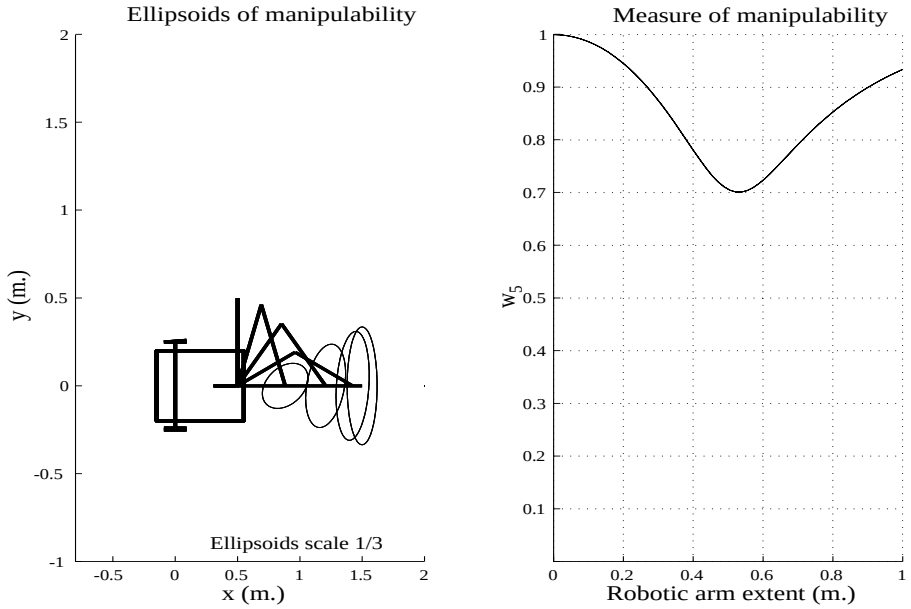

Fig. 6. Manipulability analysis for the mobile manipulator, when $\beta_3 = \frac{\pi}{2}$; contribution of the platform to the mobile manipulator manipulability.

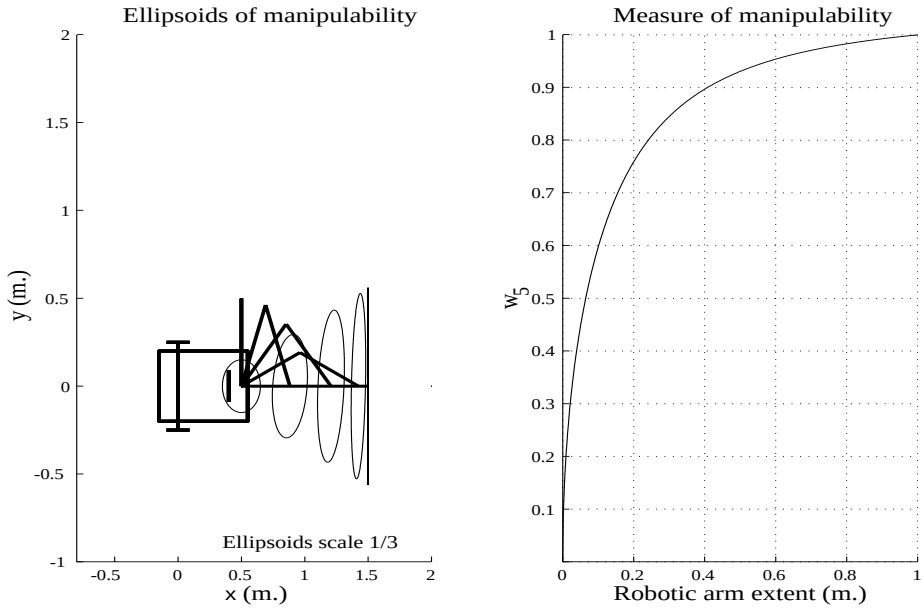

Fig. 7. Manipulability analysis for the mobile manipulator, when $\beta_3 = 0$; effects of the nonholonomic constraints on manipulability.

Thus, the mobility of the mobile manipulator is limited and this one cannot move in any direction of the operational space. This configuration can be called singular kinematic configuration (Fourquet and Renaud 1996). We also notice that the configuration corresponding to $q_{a_1} = \frac{\pi}{2}$ and $q_{a_2} = -\frac{\pi}{2}$ is no longer singular.

4. Applications to Mobile Manipulator Control

Up to now, the applications of manipulability of the whole system are very few. To our knowledge, they present the extension of manipulability for a particular mobile manipulator, for which the platform has two independent driven wheels. The applications evoked deal with the design of the mobile manipulator. Gardner and Velinsky (2000) introduce numeric comparisons that allow them to choose the position of the arm base on the platform (i.e., the values of the parameters a and b), given a robot structure (a three-joint anthropomorphic robotic arm mounted on a wheeled mobile platform) and a particular task (straight-line path on a highway). Yamamoto and Yun (1999) normalize the manipulability to evaluate the effects of maximum linear velocity of the platform on manipulability of the system. This can be useful to size the platform motoring.

In this paper, we propose to use the mobile manipulator manipulability to solve the operational motion planning problem. The use of manipulability in the generation of mobile manipulators motions was first addressed by Yamamoto and Yun (1994). These authors used the robotic arm manipulability to define preferred configurations of the robotic arm. We first developed the use of mobile manipulators manipulability in motion generation in Bayle, Fourquet, and Renaud (2001c).

4.1. Operational Motion Planning Problem

We consider the *operational motion planning problem*. From now on, we suppose that the mobile manipulators have no steering wheel, i.e., $N_s = 0$ (see the remark at the end of the paragraph). The maneuvrability control of the mobile manipulator thus reduces to its mobility control, i.e., $\boldsymbol{u} = \boldsymbol{\eta}$ and $\delta_M = \delta_m$. Also we suppose that the problem, mobile manipulator and task, is redundant, i.e., $\delta_m > m$.

For a given operational motion $\boldsymbol{\xi}^*(t)$, the problem is to find the mobility control $\boldsymbol{\eta}(t)$ such that $\boldsymbol{\xi}^*(t) = \bar{J}(t)\boldsymbol{\eta}(t)$ which asymptotically stabilizes the operational error $\boldsymbol{e}(t) = \boldsymbol{\xi}^*(t) - \boldsymbol{\xi}(t)$. The matrix $\bar{J}(t)$ is $m \times \delta_m$. We suppose that the rank of this matrix is m (this is the case in practice). Then, the previous linear system is *consistent*[4] and all the *exact* solutions are given by

$$\boldsymbol{\eta}(t) = \bar{J}^+(t)\dot{\boldsymbol{\xi}}^*(t) + \left(I_{\delta_m} - \bar{J}^+(t)\bar{J}(t)\right)\boldsymbol{g}(t),$$

4. The system $\boldsymbol{\xi}^*(t) = \bar{J}(t)\boldsymbol{\eta}(t)$ is consistent if rank $[\bar{J}(t) \mid \boldsymbol{\xi}^*(t)] =$ rank$\bar{J}(t)$.

in which $\bar{J}^+(t)$ is the pseudo-inverse of $\bar{J}(t)$ (Golub and Van Loan 1996) and $\boldsymbol{g}(t)$ any δ_m-dimensional vector. This solution minimizes the Euclidean norm $||\boldsymbol{\eta} - \boldsymbol{g}||$. Moreover, in order to asymptotically stabilize the error $\boldsymbol{e}(t)$, we can choose

$$\boldsymbol{\eta}(t) = \bar{J}^+(t)\left[\dot{\boldsymbol{\xi}}^*(t) + W\left(\boldsymbol{\xi}^*(t) - \boldsymbol{\xi}(t)\right)\right] + \left(I_{\delta_m} - \bar{J}^+(t)\bar{J}(t)\right)\boldsymbol{g}(t), \tag{14}$$

in which W is an $m-$order definite positive matrix. The previous control (14) leads to the asymptotic stability of the transient error $\boldsymbol{e}(t)$, as it verifies

$$\dot{\boldsymbol{e}}(t) + W\boldsymbol{e}(t) = 0,$$

with $\bar{J}^+(t)$ being a right-inverse of $\bar{J}(t)$.

Using eq. (12), we recall that $\dot{\boldsymbol{q}}(t) = S(t)\boldsymbol{\eta}(t)$; then, eq. (14) is written as

$$\dot{\boldsymbol{q}}(t) = S(t)\bar{J}^+(t)\left[\dot{\boldsymbol{\xi}}^*(t) + W\left(\boldsymbol{\xi}^*(t) - \boldsymbol{\xi}(t)\right)\right] + S(t)\left(I_{\delta_m} - \bar{J}^+(t)\bar{J}(t)\right)\boldsymbol{g}(t). \tag{15}$$

In eq. (15) the first term is due to the input and the second is called the *internal motion*. We can use the problem redundancy to propose a coordination strategy for the internal motion. For instance, it is interesting to avoid great variations of the generalized coordinates q_i. This can be done by a gradient descent method in which the potential function has its minimum value corresponding to the user requirements. Let $\mathcal{P}$ be a scalar function depending on the mobile manipulator configuration $\boldsymbol{q}(t)$. We can write

$$\dot{\mathcal{P}}(t) = \nabla^{\mathrm{T}}\mathcal{P}(\boldsymbol{q}(t))\dot{\boldsymbol{q}}(t),$$

where $\nabla\mathcal{P}(\boldsymbol{q}(t))$ is the gradient of the function $\mathcal{P}(\boldsymbol{q}(t))$. If we consider only the internal motion, then

$$\dot{\mathcal{P}}(t) = \nabla^{\mathrm{T}}\mathcal{P}(\boldsymbol{q}(t))S(t)\left(I_{\delta_m} - \bar{J}^+(t)\bar{J}(t)\right)\boldsymbol{g}(t).$$

In order to decrease $\mathcal{P}$, that is $\dot{\mathcal{P}}(t) \leq 0$, we propose the choice

$$\boldsymbol{g}(t) = -K\left(\nabla^{\mathrm{T}}\mathcal{P}(\boldsymbol{q}(t))S(t)\left(I_{\delta_m} - \bar{J}^+(t)\bar{J}(t)\right)\right)^{\mathrm{T}},$$

where K is a positive scalar. Indeed, with this choice

$$\dot{\mathcal{P}}(t) = -K\left[\nabla^{\mathrm{T}}\mathcal{P}(\boldsymbol{q}(t))S(t)\left(I_{\delta_m} - \bar{J}^+(t)\bar{J}(t)\right)\right]\left[\nabla^{\mathrm{T}}\mathcal{P}(\boldsymbol{q}(t))S(t)\left(I_{\delta_m} - \bar{J}^+(t)\bar{J}(t)\right)\right]^{\mathrm{T}},$$

and then $\dot{\mathcal{P}}(t) \leq 0$. Finally, the mobility control is

$$\boldsymbol{\eta}(t) = \bar{J}^+(t)\left[\dot{\boldsymbol{\xi}}^*(t) + W\left(\boldsymbol{\xi}^*(t) - \boldsymbol{\xi}(t)\right)\right] - KS(t)\left(I_{\delta_m} - \bar{J}^+(t)\bar{J}(t)\right)\left[S(t)\left(I_{\delta_m} - \bar{J}^+(t)\bar{J}(t)\right)\right]^{\mathrm{T}}.$$

This approach can be applied with various choices for $\mathcal{P}$. Hereafter, we explain how it can be applied by taking $\mathcal{P}$ as a manipulability measure.

REMARK. The control of a mobile manipulator with steering wheels is a difficult problem. When the system has one or several steering wheels, a first solution to generate the control of maneuvrability of the mobile manipulator could be to use the control scheme given in this paper to compute the control of mobility and then to compute the control of steerability independently. Indeed, as the operational velocity is independent from the control of steerability (see eq. (11)), it can be synthesized independently. A non-generic strategy has been applied successfully in Bayle (2001) for a mobile manipulator with a car-like platform. Nonetheless, solving the problem of control with a higher generality is still the object of our current research.

4.2. Using Mobile Manipulator Manipulability Measure

Two elements must be taken into account to use manipulability as a function to be optimized.

- The analytical expression of the manipulability is complex even for a simple mobile manipulator. It may not be helpful to design the $\mathcal{P}$ function. Rather, it would be more interesting to consider functions of manipulability with minimum corresponding to optimal configurations, such as $(-w)$ or w_5, and to compute their numerical gradient.

- Through our previous results (Section 3.2), the *mobile manipulator* manipulability measure has been defined in a way similar to that of the arm. Yet, depending on the application we may have to consider the whole system manipulability or only the robotic arm manipulability (for instance, when the mobile manipulator is not used in a coordinated fashion strategy). If the user wants to keep the platform motionless to manipulate with the arm alone, it would be convenient to reach the operating site in a good configuration for the arm, from a manipulation point of view. Also, both manipulability definitions can be useful for the same task. They can be taken into account by modifying the coordination strategy through the choice of a new function $\mathcal{P}$. This is a convex combination of two functions based on the arm manipulability, $\mathcal{P}_a$, and the mobile manipulator manipulability, $\mathcal{P}_{p+a}$.

In the following, we report on the results obtained for two different tasks. For both of these, only the planar position of the EE is imposed. From case to case, we choose:

- the w_5 manipulability measure, whose value decreases with isotropy of EE admissible velocities;

- Yoshikawa's manipulability measure with opposite sign $(-w)$ whose value decreases when the system moves away from singular configurations.

4.2.1. Use of the Mobile Manipulator Manipulability Measure w_5

Figure 8 illustrates the tracking of an operational motion, the associated path of which is elliptic (see also Extension 4). Here, the global manipulability of the mobile manipulator is considered through the choice of w_5 measure.

After a transient phase, the EE follows its imposed motion. It is worth noting that, during the greater part of the motion, the manipulability ellipse is very similar to a circle; the w_5 manipulability measure with respect to the subset of the considered operational coordinates—position coordinates in the plane—is minimized (see also Extension 5).

4.2.2. Combined Use of Arm and Mobile Manipulator Manipulability Measures

It is interesting to leave the user free to choose the relative weighting of manipulability measures (robotic arm and mobile manipulator measures). In fact, depending on the task at hand, we may need to use both types of measure. Let us take the example of a mobile manipulator that must first realize a coordinated operational task and then manipulate in a narrow zone. In this latter zone, moving the platform may be unsuitable and it is interesting to manipulate only with the arm. In this case, it will be interesting to consider the robotic arm manipulability. The influence of both tasks can be taken into account by using a function that is written:

$$\mathcal{P} = \alpha(\boldsymbol{\xi}^*)\mathcal{P}_{p+a} + (1 - \alpha(\boldsymbol{\xi}^*))\mathcal{P}_a.$$

It is a convex combination of the arm manipulability measure $\mathcal{P}_a$ and of that of the mobile manipulator $\mathcal{P}_{p+a}$ where the function $\alpha(\boldsymbol{\xi}^*) \in [0\ 1]$ is a cubic polynomial. This function allows us to adapt the criterion to the mobile manipulator configuration or to the EE location. *Thus, we do not use a multi-criteria function, but a transition from a criterion to another one.* Such a choice is illustrated by Figure 9.

The mobile manipulator moves in free space, from a control mode where its manipulability is taken into account (zone 1) to another control mode where the arm manipulability is taken into account (zone 3). It can be remarked that the arm manipulability may be poor whereas the whole system keeps a good measure of manipulability (see Figure 9, zone 1). This emphasizes that the choice of the manipulability is task-dependent. If the task implies to optimize manipulability in a special direction of the operational space, for instance along the reference motion of the EE, it can be achieved easily by maximizing the projection of the ellipsoid of manipulability in this direction.

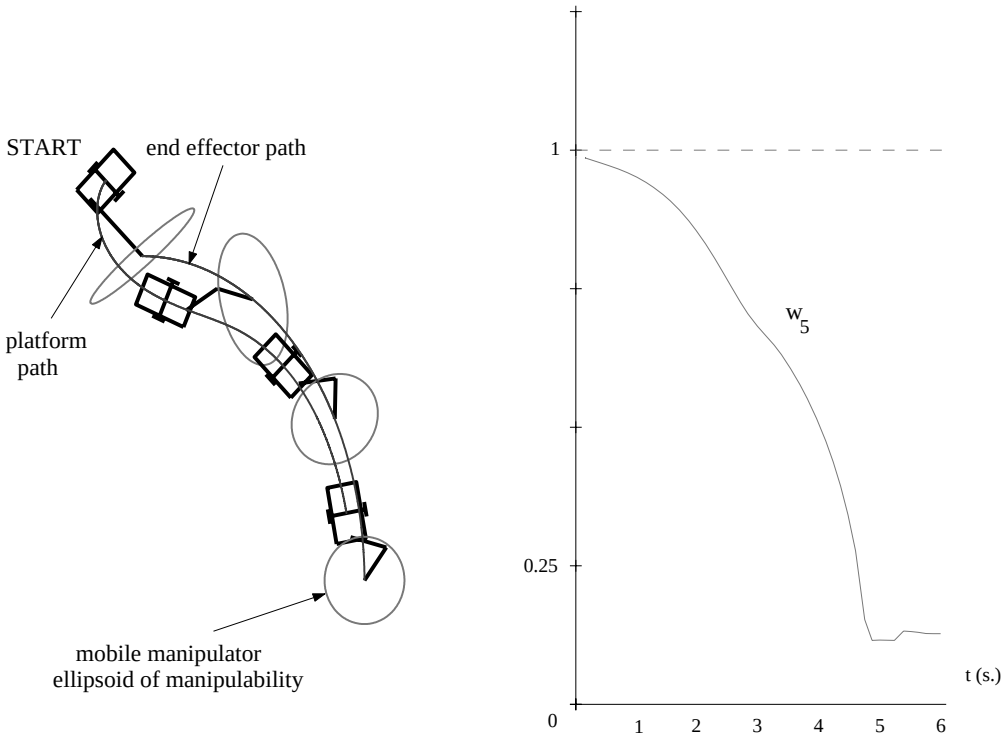

Fig. 8. Tracking an operational motion with an elliptic path.

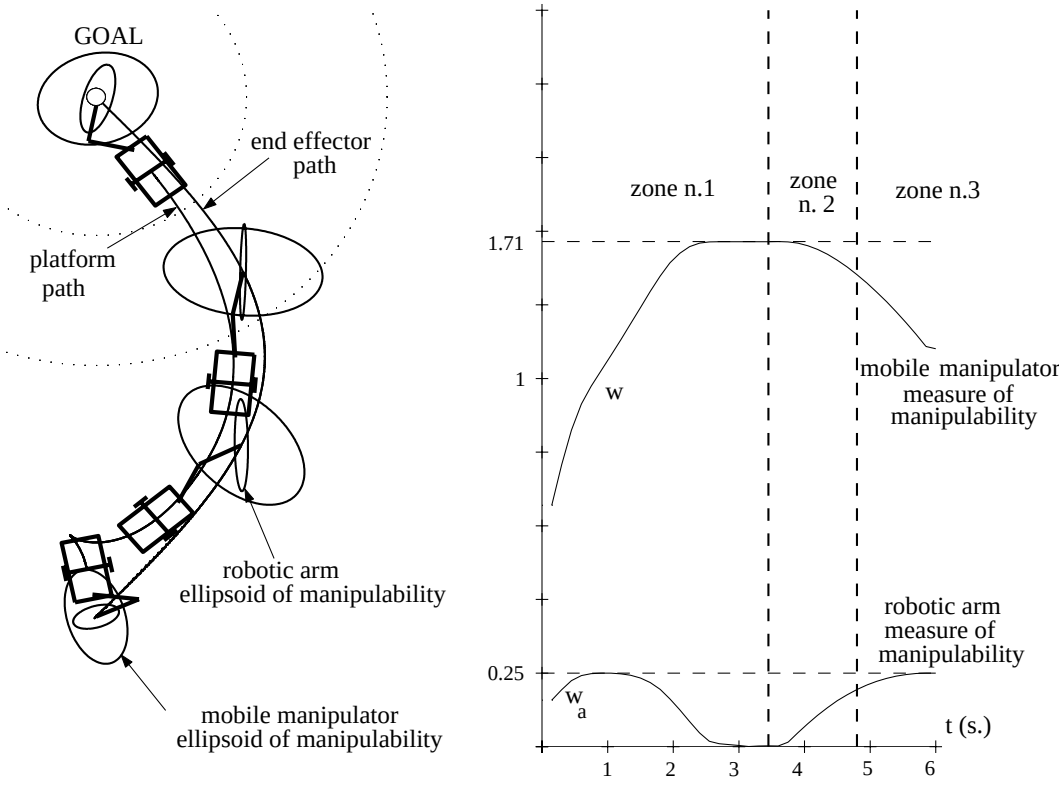

Fig. 9. Convex combination of manipulability measures.

5. Conclusion

In this paper, we have first proposed a systematic modeling of mobile manipulators built from a robotic arm mounted on a wheeled mobile platform. To this purpose, we have taken into account the nonholonomic constraints due to the rolling without slipping of the wheels on the ground. We have restricted our presentation to the kinematic and instantaneous kinematic models. Nevertheless, it would be interesting in the future to extend this work to problems with dynamic modeling. We plan to address this issue in the same generic way.

Then, we have extended the classical notion of manipulability proposed by Yoshikawa for robotic arms to the case of mobile manipulators. We have pointed the interest of this new notion for various requirements: optimal positioning of the robotic arm on the platform, design of the system itself, sizing of the platform motoring.

Finally, we have shown the advantages of this new notion for the planning of the EE motions. We have underlined the benefits for the user of choosing adequately the relative weightings of the robotic arm and of the whole mobile manipulator measures of manipulability. Various simulations (and animations; see Extensions) prove the efficiency of our operational motion planning method, which can also be applied, without difficulties, in the presence of obstacles.

Appendix: Index to Multimedia Extensions

The multimedia extension page is found at http://www.ijrr.org.

Table of Multimedia Extensions

Extension	Type	Description
1	Simulation (mpeg)	Manipulability ellipsoids for a two-revolute joint planar robotic arm.
2	Simulation (mpeg)	Manipulability ellipsoids for a planar mobile manipulator built from a car-like platform and a two-revolute joint planar robotic arm (front wheel parallel to the longitudinal axis of the platform); contribution of the mobile platform to the mobile manipulator manipulability.
3	Simulation (mpeg)	Manipulability ellipsoids for a planar mobile manipulator built from a car-like platform and a two-revolute joint planar robotic arm (front wheel orthogonal to the longitudinal axis of the platform); effects of the nonholonomic constraints on manipulability.
4	Simulation (mpeg)	Tracking of an operational motion with elliptic path while minimizing the eccentricity of the ellipsoids of manipulability.
5	Plot (pdf)	Three-dimensional plot of the path followed by the point with coordinates $[q_{a_1}\ q_{a_2}]^{\mathrm{T}}$ on the w_5 surface (this corresponds to Extension 4).
6	Simulation (mpeg)	Tracking of an operational motion while maximizing a convex combination of the manipulability measures of the robotic arm and the mobile manipulator.

Acknowledgments

This work was supported by the ROBEA program of French CNRS within the project *Control of Nonholonomic Mobile Manipulators*.

References

Arai, T. November 1996. Robots with integrated locomotion and manipulation and their future. In *IROS'96*, Osaka, Japan, pp. 541–545.

Bayle, B. 2001. Modélisation et commande cinématiques des manipulateurs mobiles à roues, PhD Thesis, LAAS–CNRS, Toulouse University.

Bayle, B., Fourquet, J.-Y., and Renaud, M. March 2000a. Manipulateurs mobiles: problématiques et état de l'art. Technical Report no 00087, LAAS–CNRS, Toulouse, France.

Bayle, B., Fourquet, J.-Y., and Renaud, M. July 2000b. A coordination strategy for mobile manipulation. In *IAS'00*, Venice, Italy, pp. 981–988.

Bayle, B., Fourquet, J.-Y., and Renaud, M. 2001a. Génération des mouvements des manipulateurs mobiles: Etat de l'art et perspectives. *Journal Européen des Systèmes Automatisés* 35(6):809–845.

Bayle, B., Fourquet, J.-Y., and Renaud, M. May 2001b. Manipulability analysis for mobile manipulators. In *ICRA'01*, Seoul, Korea, pp. 1251–1256.

Bayle, B., Fourquet, J.-Y., and Renaud, M. June 2001c. Using manipulability with nonholonomic mobile manipulators. In *International Conference on Field and Service Robotics*, Helsinki, Finland, pp. 343–348.

Bayle, B., Fourquet, J.-Y., and Renaud, M. October 2002. Kinematic control of wheeled mobile manipulators. In *IROS'02*, Lausanne, Switzerland, pp. 1572–1577.

Brock, O., and Khatib, O. October 1997. Elastic strips: Real-time path modification for mobile manipulation. In *ISRR'97*, Hayama, Japan, pp. 117–122.

Cameron, J. M., MacKenzie, D. C., and Ward, K. R. May 1993. Reactive control for mobile manipulators. In *ICRA'93*, Atlanta, USA, pp. 228–235.

Campion, G., Bastin, G., and D'Andréa-Novel, B. 1996. Structural properties and classification of kinematic and dynamic models of wheeled mobile robots. *IEEE Transactions on Robotics and Automation* 12(1):47–62.

Carriker, W. F., Khosla, P. K., and Krogh, B. H. 1991. Path planning for mobile manipulators for multiple task execution. *IEEE Transactions on Robotics and Automation* 7(3):403–408.

Chen, M., and Zalzala, A. M. S. 1997. A genetic approach to motion planning of redundant mobile manipulator systems considering safety and configuration. *Journal of Robotic Systems* 14(7):529–544.

Chong, N. Y., Yokoi, K., Oh, S.-R., and Tanie, K. April 1997. Position control of a collision tolerant passive mobile manipulator with base suspension characteristics. In *ICRA'97*, Albuquerque, USA, pp. 594–599.

Chung, J., Velinsky, S., and Hess, R. 1998. Interaction control of a redundant mobile manipulator. *International Journal of Robotics Research* 17(12):1302–1309.

Craig, J. J. 1989. *Introduction to Robotics: Mechanics and Control*, Addison-Wesley, Reading, MA.

Desai, J. P., and Kumar, V. 1996. Optimal motion plans for cooperating nonholonomic mobile manipulators in an environment with obstacles. Technical Report no 403, GRASP Laboratory, University of Pennsylvania, Philadelphia, USA.

Desai, J. P., Wang, C. C., Zefran, M., and Kumar, V. April 1996. Motion planning for multiple mobile manipulators. In *ICRA'96*, Minneapolis, USA, pp. 2073–2078.

Dong, W., Xu, Y., and Wang, Q. April 2000. On tracking control of mobile manipulators. In *ICRA'00*, San Francisco, USA, pp. 3455–3460.

Dubowsky, S., and Tanner, A. B. 1988. A study of the dynamics and control of mobile manipulators subjected to vehicle disturbances. In *Robotics Research: 4th International Symposium*, pp. 111–117.

Foulon, G., Fourquet, J.-Y., and Renaud, M. October 1998. Planning point-to-point paths for non-holonomic mobile manipulators. In *IROS'98*, Victoria, Canada, pp. 374–379.

Foulon, G., Fourquet, J.-Y., and Renaud, M. 1999. Coordinating mobility and manipulation using non-holonomic mobile manipulators. *Control Engineering Practice* 7:391–399.

Fourquet, J.-Y., and Renaud, M. 1996. Contribution à la génération de trajectoires pour un système mécanique constitué d'une plate-forme mobile non-holonome et d'un bras manipulateur. Technical Report no 96501, LAAS–CNRS, Toulouse, France.

Fourquet, J.-Y., and Renaud, M. March 1999. Coordinated control of a non-holonomic mobile manipulator. In *ISER'99*, Sydney, Australia, pp. 115–125.

Fukuda, T., Fujisawa, Y., Muro, E., Hoshino, H., Otubo, K., Uehara, K., Kosuge, K., Arai, F., and Miyazaki, T. May 1992. Manipulator/vehicle system for man–robot cooperation. In *ICRA'92*, Nice, France, pp. 74–79.

Gardner, J., and Velinsky, S. 2000. Kinematics of mobile manipulators and implications for design. *Journal of Robotic Systems* 17(6):309–320.

Golub, G., and Van Loan, C. 1996. *Matrix Computations*, Johns Hopkins University Press.

Hashimoto, M., Oba, F., and Zenitani, S. May 1995. Object-transportation control by multiple wheeled vehicle-planar Cartesian manipulator systems. In *ICRA'95*, Nagoya, Japan, pp. 2267–2272.

Hootsmans, N. A. M., and Dubowsky, S. April 1991. Large motion control of mobile manipulators including vehicle suspension characteristics. In *ICRA'91*, Sacramento, USA, pp. 2336–2341.

Huang, Q., Sugano, S., and Tanie, K. May 1998. Motion planning of a mobile manipulator considering stability and task constraints. In *ICRA'98*, Leuven, Belgium, pp. 2192–2198.

Huang, Q., Sugano, S., and Tanie, K. 2000. Coordinated motion planning for a mobile manipulator considering stability and manipulation. *International Journal of Robotics Research* 19(8):732–742.

Inoue, K., Miyamoto, T., and Okawa, Y. November 1996. Impedance control of mobile manipulator with the stability to external forces. In *IROS'96*, Osaka, Japan, pp. 721–728.

Khalil, W., and Kleinfinger, J. 1986. A new geometric notation for open and closed loop robots. In *ICRA'86*, pp. 75–79.

Khatib, O. December 1997. Mobile manipulators: Expanding the frontiers of robot applications. In *International Conference on Field and Service Robotics*, Canberra, Australia, pp. 14–17.

Khatib, O., Yokoi, K., Chang, K., Ruspini, D., Holmberg, R., and Casal, A. 1996. Coordination and decentralized cooperation of multiple mobile manipulators. *Journal of Robotic Systems* 13(11):755–764.

Lee, J.-K., Kim, S. H., and Cho, H. S. November 1996. Motion planning for a mobile manipulator to execute a multiple point-to-point task. In *IROS'96*, Osaka, Japan, pp. 737–742.

Lipkin, H., and Duffy, J. 1988. Hybrid twist and wrench control for a robotic manipulator. *ASME Journal of Mechanisms, Transmissions, and Automation in Design* 110:138–144.

Liu, K., and Lewis, F. May 1990. Decentralized continuous robust controller for mobile robots. In *ICRA'90*, Cincinnati, USA, pp. 1822–1826.

Neimark, J., and Fufaev, N. 1972. *Dynamics of Nonholonomic Systems*, Vol. 33. Translations of Mathematical Monographs.

Paul, R. 1981. *Robot Manipulators : Mathematics, Programming, and Control*, MIT Press, Cambridge, MA.

Pavlov, V., and Timofeyev, A. 1976. Construction and sta-

bilization of programmed movements of a mobile robot-manipulator. *Engineering Cybernetics* 14(6):70–79.

Pin, F. G., and Culioli, J.-C. July 1990. Multi-criteria position and configuration optimization for redundant platform/manipulator systems. In *IEEE Workshop on Intelligent Robots and Systems*, pp. 103–107.

Pin, F. G., Culioli, J.-C., and Reister, D. B. 1994. Using minimax approaches to plan optimal task commutation configurations for combined mobile platform-manipulator systems. *IEEE Transactions on Robotics and Automation* 10(1):44–54.

Pin, F. G., Hacker, C. J., Gower, K. B., and Morgansen, K. A. April 1997. Including a non-holonomic constraint in the Full Space Parametrization method for mobile manipulators motion planning. In *ICRA'97*, Albuquerque, USA, pp. 2914–2919.

Pissard-Gibolet, R. 1993. Conception et Commande par Asservissement Visuel d'un Robot Mobile, PhD Thesis, Ecole Nationale Supérieure des Mines de Paris, Sophia-Antipolis.

Quinlan, S. December 1994. Real-Time Path Modification of Collision-Free Paths, PhD Thesis, Stanford University, USA.

Rey, D. A., and Papadopoulos, E. G. April 1997. On-line automatic tip-over prevention for mobile manipulators. In *ICRA'97*, Albuquerque, USA, pp. 1273–1278.

Sciavicco, L., and Siciliano, B. 2000. *Modeling and Control of Robot Manipulators*, Springer-Verlag, Berlin.

Seraji, H. May 1993. An on-line approach to coordinated mobility and manipulation. In *ICRA'93*, Atlanta, USA, pp. 28–35.

Seraji, H. 1998. A unified approach to motion control of mobile manipulators. *International Journal of Robotics Research* 17(2):107–118.

Sugar, T., and Kumar, V. May 1999. Multiple cooperating mobile manipulators. In *ICRA'99*, Detroit, USA, pp. 15–38.

Tchoń, K., and Muszyński, R. April 2000. Instantaneous kinematics and dexterity of mobile manipulators. In *ICRA'00*, San Francisco, USA, pp. 2493–2498.

Yamamoto, Y., and Yun, X. 1994. Coordinating locomotion and manipulation of a mobile manipulator. *IEEE Transactions on Robotics and Automation* 39(6):1326–1332.

Yamamoto, Y., and Yun, X. 1996. Effect of the dynamic interaction on coordinated control of mobile manipulators. *Transactions on Robotics and Automation* 12(5):816–824.

Yamamoto, Y., and Yun, X. 1997. A modular approach to dynamic modeling of a class of mobile manipulators. *International Journal of Robotics and Automation* 12(2):41–48.

Yamamoto, Y., and Yun, X. May 1999. Unified analysis on mobility and manipulability of mobile manipulators. In *ICRA'99*, Detroit, USA, pp. 1200–1206.

Yoshikawa, T. 1985. Manipulability of robotic mechanisms. *International Journal of Robotics Research* 4(2):3–9.

Yoshikawa, T. 1990. *Foundations of Robotics: Analysis and Control*, MIT Press, Cambridge, MA.

Zhao, M., Ansari, N., and Hou, E. S. H. 1994. Mobile manipulator path planning by a genetic algorithm. *Journal of Robotic Systems* 11(3):143–153.